NIH Public Access
Author Manuscript
Semin Radiat Oncol. Author manuscript; available in PMC 2009 April 1.

Published in final edited form as:
Semin Radiat Oncol. 2008 April ; 18(2): 136–148.

Targeted Molecular Imaging in Oncology: Focus on Radiation Therapy

Sridhar Nimmagadda[1], **Eric C. Ford**[2], **John W. Wong**[2], and **Martin G. Pomper**[1]

1 *Russell H. Morgan Department of Radiology and Radiological Sciences, Johns Hopkins Medical Institutions, Baltimore, Maryland, 21231*

2 *Department of Radiation Oncology & Molecular Radiation Sciences, The Sidney Kimmel Comprehensive Cancer at Johns Hopkins, Baltimore, MD 21231*

Abstract

Anatomically based technologies (CT, MR, etc.) are in routine use in radiotherapy for planning and assessment purposes. Even with improvements in imaging, however, radiotherapy is still limited in efficacy and toxicity in certain applications. Further advances may be provided by technologies that image the molecular activities of tumors and normal tissues. Possible uses for molecular imaging include better localization of tumor regions and early assay for the radiation response of tumors and normal tissues. Critical to the success of this approach is the identification and validation of molecular probes that are suitable in the radiotherapy context. Recent developments in molecular imaging probes and integration of functional imaging with radiotherapy are promising. This review focuses on recent advances in molecular imaging strategies and probes that may aid in improving the efficacy of radiotherapy.

Introduction

The last few decades have seen a remarkable change in our understanding of the genetic, molecular and cellular basis of disease. With this new understanding there has been a shift in the management of cancer from an organ-system approach to targeting specific molecular abnormalities. Until a decade ago our understanding of cancer has been descriptive and has relied on information gathered from 10–10,000 cells at a time, collected from a heterogeneous tumor at a single instant. Recent developments in molecular imaging allow one to follow the same number of cells but the changes can be monitored dynamically. Using parametric imaging it is possible to map the variations in the architecture and physiology of disease in a three dimensional mode. This closer look at dynamic processes, however, is limited to very few cellular events because such dynamic visualization requires a clear understanding of the molecular nature of the process and the proper tools to study it.

Developments from the human genome project promise to produce more therapeutic targets. Despite this remarkable progress there has been a steady decline in the number of new agents reaching the clinic. One explanation for this is the lack of appropriate biologically relevant screens and models. Recent developments in genetic models of cancer have been addressing

Corresponding author: Martin G. Pomper, M.D., Ph.D., Johns Hopkins Medical Institutions, 1550 Orleans Street, 492 CRB II, Baltimore, MD 21231, Phone: 410-955-2789, Fax: 443-817-0990, E mail: mpomper@jhmi.edu.

Publisher's Disclaimer: This is a PDF file of an unedited manuscript that has been accepted for publication. As a service to our customers we are providing this early version of the manuscript. The manuscript will undergo copyediting, typesetting, and review of the resulting proof before it is published in its final citable form. Please note that during the production process errors may be discovered which could affect the content, and all legal disclaimers that apply to the journal pertain.

NIH-PA Author Manuscript
NIH-PA Author Manuscript
NIH-PA Author Manuscript

NIH-PA Author Manuscript

NIH-PA Author Manuscript

NIH-PA Author Manuscript

this problem. Many excellent reviews on this issue exist (1–4). Another reason is the lack of accurate prognostic markers and a way to monitor them. Imaging may enable more rapid translation of promising therapeutic agents to the clinic by demonstrating that drugs that are destined to fail are identified early and inexpensively in the development process and by enabling selection of appropriate patients, i.e., those with a phenotype that may benefit from the targeted agent, on whom to initiate clinical trials.

Recent advances in small animal imaging now allow highly specific and sensitive detection of cellular and molecular events non-invasively. Molecular imaging modalities such as positron emission tomography (PET) and single photon emission computed tomography (SPECT) provide spatial resolutions on the order of 1–2 mm. With anatomic small animal imaging modalities such as magnetic resonance imaging (MRI) and computed tomography (CT) it is possible to achieve spatial resolutions on the order of 50 μm. Significant advancements have been made clinically as well, particularly in the area of hybrid technologies such as PET-CT and SPECT-CT, which allow CT to complement the low resolution molecular imaging techniques. The details of multimodality imaging devices and their clinical and preclinical applications are beyond the scope of this review but have been addressed in detail elsewhere (5–9).

While developments in generating imaging targets and in imaging technology improve our understanding of biology, there is an unmet need in the development and characterization of new imaging probes and reagents for specific biological processes. Also, there is a strong interest in using molecular imaging not only in drug development but also in targeted treatment planning and monitoring – including image-guided radiation therapy. In this article we will focus on the current paradigms for targeted multimodality molecular imaging and their relevance to monitoring radiotherapy for cancer.

Metabolism

The classical PET radiotracer used in the clinic is [^{18}F]2-fluoro-2-deoxy-$_D$-glucose (FDG). Many tumors are known to have high glycolytic rates compared to normal tissue (10). FDG exploits that abnormal increase in glucose metabolism to image tumors. FDG is transported into tumor cells in increased amounts as a result of the upregulation of glucose transport proteins, i.e., GLUT1 and rate-limiting enzymes, e.g., hexokinase. Once inside the cell, FDG is phosphorylated into FDG-6-phosphate but does not undergo glycolysis due to the presence of a fluorine substitution in the molecule. FDG-6-phosphate accumulates and becomes metabolically “trapped” within the cell. FDG is routinely used in the clinic for diagnosis, staging, detection of recurrent disease and monitoring therapy of cancer. Many excellent reviews on FDG use in clinical monitoring have been published in the literature (11–13). The literature indicates an 84 to 87% specificity and 88 to 93 % sensitivity of FDG-PET in various oncologic applications (13).

As with other aspects of cancer imaging, FDG-PET has been the most widely employed molecular imaging technique for applications to radiotherapy. One of the main thrusts has been to use FDG-PET to delineate tumor boundaries more accurately for treatment (14,15). This has proved particularly useful in lung tumors where a large inter-user variability is observed in some tumors due to atelectasis (16,17). The addition of FDG-PET has a strong effect on the size of the region that is identified as tumor. Compared to using CT alone, the inclusion of PET data changes the size of delineated gross tumor volumes by approximately 20% to 40% in approximately half of non-small cell lung cancer (NSCLC) patients (15). FDG-PET has also been employed for tumor definition sites such as head and neck (18,19), primary brain (20), cervical (21), rectal (22) and esophageal cancers (23) and lymphoma (24).

NIH-PA Author Manuscript

NIH-PA Author Manuscript

NIH-PA Author Manuscript

Implicit in the use of PET for target definition is the need for a robust means of delineating tumor boundaries. One widely used method is to set a voxel value threshold above which all areas are considered tumor (25). The appropriate threshold level is not known *a priori*, however, and recent studies have shown that the volume recovered is extremely sensitive to the exact threshold used (26). In other words, the extent of the tumor depends on the window and level used. Given those uncertainties, further development, such as the creation of uniform standards for quantification, is needed before PET can be used confidently to outline target volumes. One interesting avenue of investigation includes validation studies comparing pathological specimens with imaging. One recent study employed a careful alignment of pathological specimens from laryngeal cancers with FDG-PET, CT and MR images obtained prior to surgery (25). That study showed significant differences in tumor volumes between the modalities (with FDG-PET returning the largest volumes). Although all of the modalities overestimated the size of the tumor, each one also missed tumor extension into some regions. Further study is clearly required.

The second way that PET may be used in radiotherapy is as a predictor or measure of therapeutic response. In head and neck cancer significantly better local control and disease-free survival have been shown for lesions with lower standard uptake values (SUVs). SUV is defined merely as the radioactivity concentration in the tumor/injected amount/patient weight) (27–29). Decreases in SUV indicating adequate therapy have also been reported for NSCLC (30–33). FDG-PET has been used extensively to measure the response to radiotherapy in head and neck cancers (34,35), as well as in lung (31,36) and brain (37–39) tumors.

Monitoring therapy-induced changes in tumor metabolism with FDG is not without limitations. FDG accumulation can be nonspecific, particularly in cases of inflammation and infiltration of macrophages, which also readily sequester FDG due to high glucose metabolism (40). Therapy-induced cellular inflammation was shown to cause a temporary increase in FDG uptake in esophageal cancer patients treated with chemoradiotherapy (41). In addition, physiologically high normal “background” metabolic activity can render the quantification of FDG uptake difficult in some areas of the body such as brain (Figure 1). Furthermore, glucose metabolic changes may not be apparent in targeted therapies, requiring additional imaging probes to complement FDG to monitor targeted cancer treatment. On the microscopic level FDG uptake has been positively correlated with hypoxia and negatively correlated with proliferation and perfusion in an experimental model (42). It is therefore likely that FDG uptake is sensitive not only to metabolic activity but other processes as well. We explore more specific radiotracers below.

Interestingly, non-specific FDG uptake may actually be useful in some clinical situations. A recent example is a study of breast cancer lumpectomy patients in the context of adjuvant partial breast irradiation where it is often difficult to identify the lumpectomy bed on CT alone. This study showed an increased FDG uptake in the lumpectomy cavity, presumably due to inflammation (Figure 2) (43). The FDG-PET distribution can aid in the definition of the lumpectomy bed. The volume of the lumpectomy cavity as defined on PET-CT was larger than that defined on CT. A radiation treatment plan based on CT alone would not adequately treat the larger PET volume. The plan can be redesigned to cover the larger PET volume, however, while still respecting the dose constraints to normal tissues.

In addition to glucose metabolism, cancer cells also have an accelerated protein metabolism and upregulated amino acid transport, which could be monitored by labeled amino acids (44–46). Radiolabeled methionine and tyrosine analogs *O*-(2-fluoroethyl)-L-tyrosine (FET), 6-fluoro-L-*m*-tyrosine (FMT), L-3-iodo-α-methyltyrosine (IMT) have been used (47) for imaging cancer. Both methionine and IMT have demonstrated very high sensitivity and specificity in detection of various tumors, particularly brain (48,49). One of the problems associated with

NIH-PA Author Manuscript

NIH-PA Author Manuscript

NIH-PA Author Manuscript

amino acid-based imaging is the metabolism of these compounds, with generation of a plethora of radioactive metabolites that render radiotracer kinetic modeling difficult. Imaging with radiolabeled amino acids is advantageous during radiotherapy monitoring – perhaps more so than FDG-PET – due to less uptake by inflammatory tissue. That is particularly the case for brain tumors where it is critical to differentiate recurrent tumor from inflammatory and other changes due solely to radiation.

Proliferation

Cellular proliferation may be measured in many ways, including use of radiolabeled lipid precursors (50) and nucleosides (51,52). While lipid precursors tend to have more than one metabolic pathway, nucleosides, particularly thymidine and its analogs, are quite unique because they incorporate into DNA and provide a readout of DNA synthesis. Preclinical and clinical studies (53–55) of thymidine labeled with carbon-11 (20.2 min) showed rapid catabolism generating considerable amounts of recirculating radioactive metabolites making [^{11}C]thymidine impractical for routine clinical use (56–59).

Nucleosides with a substitution of fluorine at the 2′- or 3′-position of the pentose sugar are more resistant to degradation by thymidine phosphorylase. One promising agent is 3′-deoxy-3′-[^{18}F]fluorothymidine (FLT). FLT is resistant to degradation and is trapped intracellularly after phosphorylation by tightly regulated S-phase cytosolic thymidine kinase (TK1) (60,61). Studies have demonstrated correlation of FLT uptake with cellular proliferation in cells, animals and humans. FLT has been used to detect and monitor changes in proliferation using PET in various cancers including colorectal (62), brain (63), and lung (64). For example, Kenny et al. have demonstrated that early changes in proliferation in patients with breast cancer can be monitored by FLT uptake just after one week of chemotherapy and preceding any observable changes in tumor volume (65).

Sugiyama et al. have demonstrated that uptake of FLT and changes in FLT uptake after radiotherapy were more pronounced than FDG and correlated well with proliferating cell nuclear antigen (PCNA) labeling index (66). In another study Apisarnthanarax et al. demonstrated the use of FLT in detecting changes in proliferation after chemoradiotherapy in an experimental model of esophageal carcinoma (67). Yang et al. have also employed FLT to assess early response to radiation in a xenograft model and compared it to changes in FDG uptake (68). This study found a marked FLT response to single doses of radiation at early time points (1–2 days post-therapy) which were larger than those measured with FDG-PET.

Although FLT is very promising as an agent for imaging proliferation, it is not readily incorporated into DNA and therefore does not reflect the total DNA synthesis. That may be a limitation to monitor the therapeutic effectiveness of cytostatic agents. Other thymidine analogs that incorporate into DNA and therefore demonstrate the efficacy more directly such as (1-(2′-deoxy-2′-[^{18}F]fluoro-β-D-arabinofuranosyl)thymine) (FMAU) (69) and 1-(2′-deoxy-2′-[^{18}F]fluoro-1-beta-D-arabinofuranosyl)-5-bromouracil (FBAU) (70) are being investigated.

Elevated choline metabolites such as phosphocholine and phosphatidylcholine, observed in tumors are a result of increased activities of choline transporters and choline kinase associated with increased cell membrane synthesis and tumor cell proliferation (71). The highly active phospholipid metabolism of tumor cells has been targeted with [^{11}C]choline as a marker of proliferation (72). [^{11}C]Choline imaging has been applied for the detection of several cancers, particularly brain and prostate (73,74). To increase the effectiveness of lipid metabolism imaging, efforts have been made to develop [^{18}F]-labeled choline analogs (75,76). Similarly, Inhibitors of choline kinase and choline transporters such as hemicholinium-3 are being investigated as potential imaging agents (77). Despite promising initial results obtained with

NIH-PA Author Manuscript

NIH-PA Author Manuscript

NIH-PA Author Manuscript

[^{11}C]choline, there are conflicting reports on its correlation with measures of proliferation (78,79).

Significant progress has been made in using MR technology to detect the changes in tumor phospholipid metabolism (80,81). Several excellent reviews on the use of ^{1}H-, ^{13}C- and ^{31}P-MR for choline metabolite detection in cancer are available (71,82). Knowledge of phospholipid metabolism has been extended to characterize the tumor progression and radiotherapy in gliomas (83,84).

Hypoxia

Solid tumors, due to imperfect and chaotic vasculature, develop regions of low oxygen concentration regions that are hypoxic. In the majority of solid tumors hypoxia is the basis for angiogenesis, metastasis and therapy resistance – particularly radiation therapy. The ability to image hypoxia has potential therapeutic applications. One hope has been that radiation therapy can be tailored to irradiate hypoxic tumor regions preferentially (85). That could theoretically give enhanced tumor control even if the tumor only has modest hypoxic subfractions (86). One difficulty with this approach, however, is that the hypoxic regions appear to change in response to radiation even at early time points as seen in a model system (87). Work is ongoing to understand these effects in more detail.

Another possible means of exploiting hypoxic conditions is the use of a prodrug activating gene that can be specifically triggered by hypoxia-specific promoters or bioreductive drugs that could be specifically activated at low tumor oxygen concentrations (88–93). Because hypoxia is a marker for poor prognosis, using hypoxia as a diagnostic marker may also be helpful for better chemotherapeutic and radiation treatment outcomes (94).

[^{18}F]Fluoromisonidazole, or 3-[^{18}F]fluoro-1-(2′-nitro-1′-imidazolyl)-2-propanol (FMISO), accumulates in regions with $pO_2 < 10$ mm Hg and is retained in a nitroreductase dependent manner. FMISO has been evaluated in preclinical (95) and clinical settings and shows correlative variation in uptake with hypoxic status in various tumors (93,96–98). The nitrosoimidazole-based SPECT imaging probe, ^{99m}Tc-labeled 4,9-diaza-3,3,10,10-tetramethyldodecan-2,11-dione dioxime [^{99m}Tc]HL91, has also been useful in predicting hypoxia status and changes during radiotherapy (99,100).

Another hypoxia marker that has been extensively investigated is a metal chelating agent Cu-diacetyl-bis(N4-methylthiosemicarbazone) (Cu-ATSM) (101). Uptake of Cu-ATSM has reliably detected hypoxic regions within NSCLC (102) and cervical tumors and used in image-guided intensity-modulated radiation therapy (IMRT) of advanced cancers (103). However, comparison studies in murine squamous cell carcinoma and other models showed better correlation between FMISO uptake changes and hypoxia levels than Cu-ATSM (101,104). Cu-ATSM, labeled with ^{64}Cu, due to its favorable β-particle emissions, has also been used as a therapeutic agent (105–107). Studies have indicated that the Cu-ATSM uptake is particularly sensitive to the time at which images are acquired, probably due to the passive transport across cell membranes (108). A new generation of nitrosoimidazoles and labeled azomycin analogs such as [^{18}F]fluoroazomycin arabinoside (FAZA) and iodo-azomycin-galactosides (IAZG) are under investigation as PET and SPECT imaging probes to determine the predictive value of hypoxia directed treatments and chemoradiotherapy (109,110).

Apoptosis

Apoptosis, or programmed cell death, is a tightly regulated and genetically defined cellular process *in vivo*. The externalization of phosphatidylserine (PS) to the cell surface is a hallmark of the caspase-3 activated apoptotic process (111,112). Externalized PS can be detected using

NIH-PA Author Manuscript

NIH-PA Author Manuscript

NIH-PA Author Manuscript

a 40kDa vesicle protein called annexin, which has been extensively used in molecular imaging for imaging apoptosis (113–116). ^{99m}Tc-labeled annexin uptake after chemotherapy has been shown to be a predictor of tumor response and prognosis in some human cancers (117). Radiation induced apoptosis also correlates with the uptake of radiolabeled annexin in follicular lymphoma patients undergoing radiotherapy (118). Annexin labeled with near infrared optical imaging probes has also been used for tumor detection and treatment response in animal models (119,120).

Another molecule that binds to externalized PS is C2 domain of synaptotagmin (121). Synaptotagmin conjugated with SPIO nanoparticles has been used to detect apoptosis in murine lymphoma models using MRI (122).

The preceding sections have dealt with imaging agents and related mechanisms (metabolism, proliferation and hypoxia, and apoptosis) that have been studied to at least some extent in the context of radiation therapy. We now consider processes that are also amenable to the development and use of targeted imaging agents but have not yet been studied with respect to the radiation therapy, namely: receptor-based targets, gene expression and angiogenesis. These processes are clearly relevant for radiotherapy and could be used either to predict response to therapy, provide an early measure of outcome, or possibly allow tailored therapy *via* dynamic measurements.

Receptor-based imaging

Receptors play a pivotal role in signal transduction and proliferation (123,124). Expression levels of estrogen receptor (ER) are regularly used for prognosis in patients with breast cancer and to predict who will respond favorably to endocrine therapy (125). [^{18}F]Fluoroestrodiol (FES), a ligand that binds ER, has been shown to predict response to endocrine therapy (126). Dehdashti et al. found that FES-PET imaging was useful in predicting the ultimate response to tamoxifen treatment within 7 to 10 days of initiating this form of endocrine therapy (127). Similarly, androgen-dependent prostate carcinomas can be screened for androgen receptor status with the PET imaging agent, [^{18}F]fluoro-dihydroxytestosterone (FDHT)(128), with promising initial clinical results.

Growth factor receptors such as epidermal growth factor receptor (EGFR) are also becoming viable imaging targets. EGFR is overexpressed in NSCLC, bladder, cervical, ovarian, kidney and pancreatic cancers. Several SPECT-, NIRF- and PET-based EGFR inhibitors and antibodies are being investigated. Promising results were demonstrated from immunoimaging with an anti-EGFR antibody in patients with NSCLC (129–131). Small molecule inhibitors of EGFR such as gefitinib and others are also being functionalized for imaging (132–134).

HER2/neu receptor is significantly overexpressed in breast, ovarian, gastric, lung, bladder, kidney and several other cancers (135). HER2/neu receptor is a predictive marker for therapy response in breast cancer patients (136). HER2/neu-based imaging agents, mainly radiolabeled antibodies, are being investigated for classification of receptor status (137). The first patient study with [^{111}In]trastuzumab allowed identification of the HER22/neu positive tumors in patients with metastatic breast cancer (138).

Neuroendocrine tumors express a high density of somatostatin receptors. Scintigraphic somatostatin receptor imaging of neuroendocrine tumors with radiolabeled somatostatin analogs such as [^{111}In]DTPA-$_D$-Phe^1-octreotide is a routine clinical diagnostic tool (139). Currently ^{68}Ga- and ^{64}Cu-labeled analogs are also being investigated as PET radiotracers (140–142) in order to take advantage of the inherently superior sensitivity of PET.

NIH-PA Author Manuscript

NIH-PA Author Manuscript

NIH-PA Author Manuscript

MR imaging of tumor receptors is rather challenging due to the combination of low concentration of such receptors and the inherent limitation of sensitivity for MR. However, novel strategies to improve signal intensity for MR-based molecular imaging have been developed to overcome this limitation. For example, tumors expressing an engineered transferrin receptor have been imaged using a superparamagnetic iron oxide (SPIO)-labeled transferrin receptor ligand (143). In another study, Artemov et al. have targeted the HER2/neu receptor overexpressed in NT-5 breast cancer cells with a two-step avidin-biotin system. In this approach animals were pretreated with a biotinylated HER2/neu antibody. After clearance of the unbound antibody streptavidin-conjugated gadalonium-chelates were administered. That approach allowed controlled signal amplification for specific detection of the HER2/neu positive tumors (144,145).

Gene expression

The future of gene therapy lies in safe and efficient delivery and controlled expression of targeted genes at the tissue of interest. Gene delivery remains a considerable challenge because of poor specificity, inadequate transfer efficiency and lack of correlation between expression and function of the genetic material introduced (146). To achieve a better therapeutic response, quantitative and noninvasive monitoring of distribution and knowledge of the magnitude and duration of gene expression are essential. To improve the assessment of gene delivery, several imaging platforms employing various reporter gene strategies and reporter probes have been explored. Some of the most common reporter gene systems based on either enzymes, receptors or transporters in nuclear imaging are 1) the sodium/iodide symporter (NIS) system with ^{131}I (147,148), 2) the wild type and mutant dopamine receptor (D_2R) system with 3-*N*-(2-[^{18}F] fluoroethyl)spiperone (^{18}F-FESP) as the imaging probe (149,150), 3) wild type herpes simplex thymidine kinase (HSV1-*tk*) system with radiolabeled analogs of 1-(2′-deoxy-2′-fluoro-1-beta-d-arabinofuranosyl)-5-iodouracil (FIAU) (151,152) and 4) mutant herpes simplex thymidine kinase (HSV1-*sr39tk*) system with 9-(4-[^{18}F]fluoro-3-hydroxymethylbutyl)guanine, [^{18}F] FHBG (153,154). By tagging an appropriate reporter gene, many cellular processes such as initiation of transcription (155), transcriptional regulation (156), translation of mRNA (157), protein-protein interactions (158), and antitumor immune response (159) etc., have been imaged.

The first imaging-based readout of human gene therapy was reported by Jacobs et al. in glioma patients undergoing stereotactic gene therapy. Imaging of the HSV-tk expression was undertaken with [^{124}I]FIAU-PET (206). Only one out of the five patients showed an indication of radiotracer accumulation due to transgene expression. In another study Peñuelas et al. monitored HSV-tk expression in patients with hepatocellular carcinoma after an intratumoral injection of a recombinant adenovirus. The gene expression levels monitored using [^{18}F]FHBG showed a viral dose-dependent accumulation of the radiotracer (160).

Instead of using an exogenous reporter gene system, Fu et al. utilized the viral thymidine kinase expression in Epstein-Barr virus and other gammaherpesvirus-associated tumors in a preclinical model system. The authors induced the viral TK expression using bortezomib and monitored the expression levels with [^{125}I]FIAU-SPECT (Figure 3). This mechanistic approach may be useful in targeting radiolabeled and therapeutic agents to virus-associated tumors (161).

Hypoxia induces a number of genes and is a significant contributor to the radiation resistance observed during cancer treatment (162). Greco et al. have successfully achieved a therapeutic gain *in vitro* by employing vectors containing hypoxia responsive elements and radiation-responsive CArG elements from the *Egr1* early growth response gene. This novel strategy utilizes the adverse gene expression triggered in response to hypoxia and/or ionizing radiation stimuli (89,163). The effectiveness of these combined therapies *in vivo* are yet to be determined.

NIH-PA Author Manuscript

NIH-PA Author Manuscript

NIH-PA Author Manuscript

MR-based gene expression imaging is still in its infancy with only a few endogenous reporter genes in development (164,165). Recently Gilad et al. have developed a chemical-exchange saturation transfer (CEST)-based lysine-rich protein that could be turned on or off by selectively saturating at the exchangeable proton-resonance frequency. The authors demonstrated the ability to image CEST reporter gene stably expressed in brain xenografts using MRI (166).

Angiogenesis

Angiogenesis, the development of new blood vessels from preexisting blood vessels, is fundamental to tumor growth and transition from a benign into malignant state (167,168). As a result angiogenesis has become an important therapeutic target and several novel therapies based on either the existing tumor blood vessels (vascular disrupting agents) or tumor blood vessel development (antiangiogenic agents) have been developed (169). Since the effect of the antiangiogenic drugs seems to be primarily cytostatic, new molecular measures of biological response based on membrane proteins selectively expressed by angiogenic vessels have been explored (170). In addition, other physical parameters such as tumor vascular permeability, perfusion, blood volume, and microvessel density have been investigated with MRI, CT and PET (171–173). Some of the molecules germane to angiogenesis that have gained particular attention are vascular endothelial growth factor (VEGF), VEGF receptors (VEGFR), $\alpha_v\beta_3$ integrin, matrix metalloproteinases (MMPs) and thrombospondin-1 receptor (170,174).

VEGF, a mitogen, plays a critical role in stimulating endothelial migration, proliferation and angiogenesis (175). Thus VEGF-targeted imaging may provide valuable information on tumor angiogenesis and antiangeogenic treatments. Several VEGF isoforms ($VEGF_{121,}$ $VEGF_{165}$) were either labeled directly or tagged with chelating agents to label with positron (176) or gamma emitters (177–179) to visualize the VEGFR expression in preclinical models. Some of the most valuable information was derived from PET imaging studies of the ^{124}I-labeled humanized mouse monoclonal anti-VEGF antibody, HuMV833. This study in advanced cancers revealed a marked variation in the pathophysiologic behavior of tumors, even within the same patient, to antibody distribution, clearance and biological response demonstrating the need for a more tailored approach to using cytostatic antiangiogenic agents (180).

Integrins, a family of cell adhesion molecules, play a key role in endothelial cell migration and survival during angiogenesis. Of the family of integrins, $\alpha_v\beta_3$ integrin is significantly upregulated on activated endothelial cells during angiogenesis and interacts with extracellular matrix proteins with an exposed RGD (arginine-glycine-aspartic acid) motif such as vitronectin, fibronectin and fibrinogen (181,182). Several novel radiotracers containing RGD sequences labeled with ^{18}F, ^{64}Cu, ^{99m}Tc, ^{111}In, or ^{90}Yr to target specifically tumor integrins have shown high tumor/background ratios in preclinical models (183). Cyclic glycosylated pentapeptides labeled with ^{18}F have been successfully used to image $\alpha_v\beta_3$ integrin expression in cancer patients (Figure 4) (184,185).

Other imaging modalities have also been extensively used for integrins; MR imaging with paramagenetic nanoparticles (186), antibody coated liposomes (187) and Gd-perfluorocarbon nanoparticle-conjugated antibodies (188) have been used for targeted tumor $\alpha_v\beta_3$ imaging. Near infrared-based optical imaging agents (189) and $\alpha_v\beta_3$ targeted microbubbles for ultrasound have also been used to image tumor angiogenesis (190).

Matrix metalloproteinases, a class of Zn^{+2}-dependent endopeptidases, play a crucial role in cancer cell extravasation and invasion (191,192). Of the 25 known MMPs, gelatinases (MMP-2 and 9) are preferentially detected in tumors, are capable of collagen IV degradation and are of particular interest as imaging targets. Several inhibitors of MMPs, including tissue inhibitors of MMPs and MMP-specific small molecule inhibitors labeled with several PET and gamma

NIH-PA Author Manuscript

NIH-PA Author Manuscript

NIH-PA Author Manuscript

emitting radionuclides, have been used for imaging (193,194). So far, studies in preclinical and clinical imaging with MMP inhibitors have not shown convincing MMP specific tumor uptake (195–197). In contrast to experience with radiolabeled probes, near infrared optical imaging "smart" probes designed to be activated by specific MMPs have shown MMP specific tumor uptake (198,199). Other endothelial markers such as endostatins and E-selectin are under development and show some promise (200,201).

Future of targeted molecular imaging for radiation therapy

Molecular imaging is emerging as a powerful technique in the management of cancer and radiation treatment planning. Although the collaborative effort between various science and engineering disciplines is greater now than ever before, more integration is necessary. With the exception of FDG, the imaging agents described above are largely unstudied in the context of radiation therapy. Early studies indicate that some of these compounds may be useful either for monitoring or predicting the response to radiotherapy or possibly for improving treatment planning (e.g. better tumor delineation). More studies of the properties of these agents are needed that address the radiation response and other issues relevant to radiation therapy.

Immediate clinical impact may derive from extending current chemoradiotherapy approaches to new targeted therapies, such as the use of EGFR inhibitors (202), to achieve a synergistic effect. Also, development of radiation sensitive gene therapy approaches as described in hypoxia section above, and radiation-triggered release of chemotherapeutic agents or radiation-sensitive prodrugs could pave the way for more localized treatment delivery.

From a probe development standpoint, it may be time for chemists to concentrate more on developing dual or multiple use agents to move into "theragnostic" imaging. Although radiation treatment planning using molecular imaging techniques could be considered theragnostic imaging, another meaning could incorporate true dual-use probes – that identify tissues to be treated and treat them concurrently. Such an agent may be for gene therapy, where the gene, which contains both an imaging "beacon" and therapeutic moiety, is selectively expressed within the target lesion. The use of DNA (aptamers) as a direct imaging agent has showed some promise but additional work is required (203). There is still a great need for the development and validation of targeted imaging agents and ultimately their use as treatment endpoints for therapy assessment.

Allowing the use of microdosing to assess the pharmacokinetics and pharmacodynamics of novel agents (204) and the National Cancer Institute recommending the use of "phase 0" trials for the new drug/imaging agents (205) are facilitating the rapid translation of the most promising agents. As evidenced by the proliferation of preclinical and in some cases clinical, imaging programs within the pharmaceutical industry we can anticipate further streamlining of imaging agents to the clinic. Soon we will have data to show how much money, if any, molecular imaging can save in the drug/therapeutic development process. In cases where direct imaging is not feasible, alternative strategies to image the effector pathways, as gained from preclinical experience, will be helpful in assessing the therapeutic effect of the new agents while they are still in phase 0 trials.

For molecular imaging to realize its full potential in facilitating personalized patient care, the localization of specific imaging probes will need to be correlated carefully with established prognostic markers and linked to gene and tissue arrays derived from patient specimens. Perhaps nowhere more in cancer therapy than in radiation treatment planning can molecular imaging provide guidance. Although of increasing sophistication, the anatomic imaging methods currently used will soon give way to sensitive molecular imaging techniques for providing the utmost in specific, and in many cases targeted, radiation therapy.

NIH-PA Author Manuscript

NIH-PA Author Manuscript

NIH-PA Author Manuscript

References

1. Olive KP, Tuveson DA. The use of targeted mouse models for preclinical testing of novel cancer therapeutics. Clin Cancer Res Sep 15;2006 12(18):5277–5287. [PubMed: 17000660]
2. Sharpless NE, Depinho RA. The mighty mouse: genetically engineered mouse models in cancer drug development. Nat Rev Drug Discov Sep 2006;5(9):741–754.
3. Singh M, Johnson L. Using genetically engineered mouse models of cancer to aid drug development: an industry perspective. Clin Cancer Res Sep 15;2006 12(18):5312–5328. [PubMed: 17000664]
4. Van Dyke T, Jacks T. Cancer modeling in the modern era: progress and challenges. Cell Jan 25;2002 108(2):135–144. [PubMed: 11832204]
5. Pomper MG. Molecular imaging: an overview. Acad Radiol Nov 2001;8(11):1141–1153.
6. Pomper MG. Translational molecular imaging for cancer. Cancer Imaging 2005;5 Spec No A:S16–26. [PubMed: 16361132]
7. Pomper MG, Phillips E, Fan H, et al. Synthesis and Biodistribution of Radiolabeled {alpha}7 Nicotinic Acetylcholine Receptor Ligands. J Nucl Med Feb 2005;46(2):326–334.
8. Massoud TF, Gambhir SS. Molecular imaging in living subjects: seeing fundamental biological processes in a new light. Genes Dev Mar 1;2003 17(5):545–580. [PubMed: 12629038]
9. Gelovani Tjuvajev J, Blasberg RG. In vivo imaging of molecular-genetic targets for cancer therapy. Cancer Cell Apr 2003;3(4):327–332.
10. Warburg O. On the origin of cancer cells. Science Feb 24;1956 123(3191):309–314. [PubMed: 13298683]
11. Ak I, Stokkel MP, Pauwels EK. Positron emission tomography with 2-[18F]fluoro-2-deoxy-D-glucose in oncology. Part II. The clinical value in detecting and staging primary tumours. J Cancer Res Clin Oncol 2000;126(10):560–574. [PubMed: 11043393]
12. Pauwels EK, Sturm EJ, Bombardieri E, Cleton FJ, Stokkel MP. Positron-emission tomography with [18F]fluorodeoxyglucose. Part I. Biochemical uptake mechanism and its implication for clinical studies. J Cancer Res Clin Oncol 2000;126(10):549–559. [PubMed: 11043392]
13. Gambhir SS, Czernin J, Schwimmer J, Silverman DH, Coleman RE, Phelps ME. A tabulated summary of the FDG PET literature. J Nucl Med May 2001;42(5 Suppl):1S–93S.
14. van Baardwijk A, Baumert BG, Bosmans G, et al. The current status of FDG-PET in tumour volume definition in radiotherapy treatment planning. Cancer Treat Rev Jun 2006;32(4):245–260.
15. Bradley J, Thorstad WL, Mutic S, et al. Impact of FDG-PET on radiation therapy volume delineation in non-small-cell lung cancer. Int J Radiat Oncol Biol Phys May 1;2004 59(1):78–86. [PubMed: 15093902]
16. Caldwell CB, Mah K, Ung YC, et al. Observer variation in contouring gross tumor volume in patients with poorly defined non-small-cell lung tumors on CT: the impact of 18FDG-hybrid PET fusion. Int J Radiat Oncol Biol Phys Nov 15;2001 51(4):923–931. [PubMed: 11704312]
17. Gondi V, Bradley K, Mehta M, et al. Impact of hybrid fluorodeoxyglucose positron-emission tomography/computed tomography on radiotherapy planning in esophageal and non-small-cell lung cancer. Int J Radiat Oncol Biol Phys Jan 1;2007 67(1):187–195. [PubMed: 17189070]
18. Andrade RS, Heron DE, Degirmenci B, et al. Posttreatment assessment of response using FDG-PET/CT for patients treated with definitive radiation therapy for head and neck cancers. Int J Radiat Oncol Biol Phys Aug 1;2006 65(5):1315–1322. [PubMed: 16750327]
19. Gregoire V, Bol A, Geets X, Lee J. Is PET-based treatment planning the new standard in modern radiotherapy? The head and neck paradigm. Semin Radiat Oncol Oct 2006;16(4):232–238.
20. Tralins KS, Douglas JG, Stelzer KJ, et al. Volumetric analysis of 18F-FDG PET in glioblastoma multiforme: prognostic information and possible role in definition of target volumes in radiation dose escalation. J Nucl Med Dec 2002;43(12):1667–1673.
21. Sakurai H, Suzuki Y, Nonaka T, et al. FDG-PET in the detection of recurrence of uterine cervical carcinoma following radiation therapy--tumor volume and FDG uptake value. Gynecol Oncol Mar 2006;100(3):601–607.
22. Cascini GL, Avallone A, Delrio P, et al. 18F-FDG PET is an early predictor of pathologic tumor response to preoperative radiochemotherapy in locally advanced rectal cancer. J Nucl Med Aug 2006;47(8):1241–1248.

NIH-PA Author Manuscript

NIH-PA Author Manuscript

NIH-PA Author Manuscript

23. Westerterp M, van Westreenen HL, Reitsma JB, et al. Esophageal cancer: CT, endoscopic US, and FDG PET for assessment of response to neoadjuvant therapy--systematic review. Radiology Sep 2005;236(3):841–851.
24. Kasamon YL, Jones RJ, Wahl RL. Integrating PET and PET/CT into the risk-adapted therapy of lymphoma. J Nucl Med Jan 2007;48 Suppl 1:19S–27S.
25. Erdi YE, Mawlawi O, Larson SM, et al. Segmentation of lung lesion volume by adaptive positron emission tomography image thresholding. Cancer Dec 15;1997 80(12 Suppl):2505–2509. [PubMed: 9406703]
26. Ford EC, Kinahan PE, Hanlon L, et al. Tumor delineation using PET in head and neck cancers: threshold contouring and lesion volumes. Med Phys Nov 2006;33(11):4280–4288.
27. Allal AS, Dulguerov P, Allaoua M, et al. Standardized uptake value of 2-[(18)F] fluoro-2-deoxy-D-glucose in predicting outcome in head and neck carcinomas treated by radiotherapy with or without chemotherapy. J Clin Oncol Mar 1;2002 20(5):1398–1404. [PubMed: 11870185]
28. Allal AS, Slosman DO, Kebdani T, Allaoua M, Lehmann W, Dulguerov P. Prediction of outcome in head-and-neck cancer patients using the standardized uptake value of 2-[18F]fluoro-2-deoxy-D-glucose. Int J Radiat Oncol Biol Phys Aug 1;2004 59(5):1295–1300. [PubMed: 15275712]
29. Brun E, Kjellen E, Tennvall J, et al. FDG PET studies during treatment: prediction of therapy outcome in head and neck squamous cell carcinoma. Head Neck Feb 2002;24(2):127–135.
30. Cerfolio RJ, Ojha B, Mukherjee S, Pask AH, Bass CS, Katholi CR. Positron emission tomography scanning with 2-fluoro-2-deoxy-d-glucose as a predictor of response of neoadjuvant treatment for non-small cell carcinoma. J Thorac Cardiovasc Surg Apr 2003;125(4):938–944.
31. Mac Manus MP, Hicks RJ, Matthews JP, et al. Positron emission tomography is superior to computed tomography scanning for response-assessment after radical radiotherapy or chemoradiotherapy in patients with non-small-cell lung cancer. J Clin Oncol Apr 1;2003 21(7):1285–1292. [PubMed: 12663716]
32. Rege S, Safa AA, Chaiken L, Hoh C, Juillard G, Withers HR. Positron emission tomography: an independent indicator of radiocurability in head and neck carcinomas. Am J Clin Oncol Apr 2000;23 (2):164–169.
33. Weber WA, Petersen V, Schmidt B, et al. Positron emission tomography in non-small-cell lung cancer: prediction of response to chemotherapy by quantitative assessment of glucose use. J Clin Oncol Jul 15;2003 21(14):2651–2657. [PubMed: 12860940]
34. Hautzel H, Muller-Gartner HW. Early changes in fluorine-18-FDG uptake during radiotherapy. J Nucl Med Sep 1997;38(9):1384–1386.
35. Yao M, Graham MM, Smith RB, et al. Value of FDG PET in assessment of treatment response and surveillance in head-and-neck cancer patients after intensity modulated radiation treatment: a preliminary report. Int J Radiat Oncol Biol Phys Dec 1;2004 60(5):1410–1418. [PubMed: 15590172]
36. Erdi YE, Macapinlac H, Rosenzweig KE, et al. Use of PET to monitor the response of lung cancer to radiation treatment. Eur J Nucl Med Jul 2000;27(7):861–866.
37. Charnley N, West CM, Barnett CM, et al. Early change in glucose metabolic rate measured using FDG-PET in patients with high-grade glioma predicts response to temozolomide but not temozolomide plus radiotherapy. Int J Radiat Oncol Biol Phys Oct 1;2006 66(2):331–338. [PubMed: 16839701]
38. Rozental JM, Levine RL, Mehta MP, et al. Early changes in tumor metabolism after treatment: the effects of stereotactic radiotherapy. Int J Radiat Oncol Biol Phys May 1991;20(5):1053–1060.
39. Spence AM, Muzi M, Graham MM, et al. 2-[(18)F]Fluoro-2-deoxyglucose and glucose uptake in malignant gliomas before and after radiotherapy: correlation with outcome. Clin Cancer Res Apr 2002;8(4):971–979.
40. Kubota R, Yamada S, Kubota K, Ishiwata K, Tamahashi N, Ido T. Intratumoral distribution of fluorine-18-fluorodeoxyglucose in vivo: high accumulation in macrophages and granulation tissues studied by microautoradiography. J Nucl Med Nov 1992;33(11):1972–1980.
41. Arslan N, Miller TR, Dehdashti F, Battafarano RJ, Siegel BA. Evaluation of response to neoadjuvant therapy by quantitative 2-deoxy-2-[18F]fluoro-D-glucose with positron emission tomography in patients with esophageal cancer. Mol Imaging Biol Jul 2002;4(4):301–310.

NIH-PA Author Manuscript

NIH-PA Author Manuscript

NIH-PA Author Manuscript

42. Pugachev A, Ruan S, Carlin S, et al. Dependence of FDG uptake on tumor microenvironment. Int J Radiat Oncol Biol Phys Jun 1;2005 62(2):545–553. [PubMed: 15890599]
43. Ford E, Lavely W, Frassica D, et al. Comparison of FDG-PET/CT and CT for delineation of lumpectomy cavity for partial breast irradiation, submitted. Int J Radiat Oncol Biol Phys. 2007
44. Busch H, Davis JR, Honig GR, Anderson DC, Nair PV, Nyhan WL. The uptake of a variety of amino acids into nuclear proteins of tumors and other tissues. Cancer Res Nov 1959;19:1030–1039.
45. Isselbacher KJ. Sugar and amino acid transport by cells in culture--differences between normal and malignant cells. N Engl J Med Apr 27;1972 286(17):929–933. [PubMed: 4335317]
46. Laverman P, Boerman OC, Corstens FH, Oyen WJ. Fluorinated amino acids for tumour imaging with positron emission tomography. Eur J Nucl Med Mol Imaging May 2002;29(5):681–690.
47. Jager PL, Vaalburg W, Pruim J, de Vries EG, Langen KJ, Piers DA. Radiolabeled amino acids: basic aspects and clinical applications in oncology. J Nucl Med Mar 2001;42(3):432–445.
48. Kuwert T, Morgenroth C, Woesler B, et al. Uptake of iodine-123-alpha-methyl tyrosine by gliomas and non-neoplastic brain lesions. Eur J Nucl Med Oct 1996;23(10):1345–1353.
49. Ogawa T, Shishido F, Kanno I, et al. Cerebral glioma: evaluation with methionine PET. Radiology Jan 1993;186(1):45–53.
50. Yoshimoto M, Waki A, Obata A, Furukawa T, Yonekura Y, Fujibayashi Y. Radiolabeled choline as a proliferation marker: comparison with radiolabeled acetate. Nucl Med Biol Oct 2004;31(7):859–865.
51. Mankoff DA, Shields AF, Krohn KA. PET imaging of cellular proliferation. Radiol Clin North Am Jan 2005;43(1):153–167.
52. Kenny LM, Aboagye EO, Price PM. Positron emission tomography imaging of cell proliferation in oncology. Clin Oncol (R Coll Radiol) May 2004;16(3):176–185.
53. Shields AF, Coonrod DV, Quackenbush RC, Crowley JJ. Cellular sources of thymidine nucleotides: studies for PET. J Nucl Med Sep 1987;28(9):1435–1440.
54. Quackenbush RC, Shields AF. Local re-utilization of thymidine in normal mouse tissues as measured with iododeoxyuridine. Cell Tissue Kinet Nov 1988;21(6):381–387.
55. Shields AF, Lim K, Grierson J, Link J, Krohn KA. Utilization of labeled thymidine in DNA synthesis: studies for PET. J Nucl Med Mar 1990;31(3):337–342.
56. Shields AF, Graham MM, Kozawa SM, et al. Contribution of labeled carbon dioxide to PET imaging of carbon-11-labeled compounds. J Nucl Med Apr 1992;33(4):581–584.
57. Mankoff DA, Shields AF, Graham MM, Link JM, Krohn KA. A graphical analysis method to estimate blood-to-tissue transfer constants for tracers with labeled metabolites. J Nucl Med Dec 1996;37(12): 2049–2057.
58. Shields AF, Mankoff D, Graham MM, et al. Analysis of 2-carbon-11-thymidine blood metabolites in PET imaging. J Nucl Med Feb 1996;37(2):290–296.
59. Mankoff DA, Shields AF, Graham MM, Link JM, Eary JF, Krohn KA. Kinetic analysis of 2-[carbon-11]thymidine PET imaging studies: compartmental model and mathematical analysis. J Nucl Med Jun 1998;39(6):1043–1055.
60. Sherley JL, Kelly TJ. Human cytosolic thymidine kinase. Purification and physical characterization of the enzyme from HeLa cells. J Biol Chem Jan 5;1988 263(1):375–382. [PubMed: 3335503]
61. Shields AF, Grierson JR, Dohmen BM, et al. Imaging proliferation in vivo with [F-18]FLT and positron emission tomography. Nat Med Nov 1998;4(11):1334–1336.
62. Visvikis D, Francis D, Mulligan R, et al. Comparison of methodologies for the in vivo assessment of (18)FLT utilisation in colorectal cancer. Eur J Nucl Med Mol Imaging. Nov 14;2003
63. Choi SJ, Kim JS, Kim JH, et al. [(18)F]3′-deoxy-3′-fluorothymidine PET for the diagnosis and grading of brain tumors. Eur J Nucl Med Mol Imaging. Feb 15;2005
64. Buck AK, Halter G, Schirrmeister H, et al. Imaging proliferation in lung tumors with PET: 18F-FLT versus 18F-FDG. J Nucl Med Sep 2003;44(9):1426–1431.
65. Kenny L, Coombes RC, Vigushin DM, Al-Nahhas A, Shousha S, Aboagye EO. Imaging early changes in proliferation at 1 week post chemotherapy: a pilot study in breast cancer patients with 3′-deoxy-3′-[(18)F]fluorothymidine positron emission tomography. Eur J Nucl Med Mol Imaging. Mar 2;2007

NIH-PA Author Manuscript

NIH-PA Author Manuscript

NIH-PA Author Manuscript

66. Sugiyama M, Sakahara H, Sato K, et al. Evaluation of 3′-deoxy-3′-18F-fluorothymidine for monitoring tumor response to radiotherapy and photodynamic therapy in mice. J Nucl Med Oct 2004;45(10):1754–1758.
67. Apisarnthanarax S, Alauddin MM, Mourtada F, et al. Early detection of chemoradioresponse in esophageal carcinoma by 3′-deoxy-3′-3H-fluorothymidine using preclinical tumor models. Clin Cancer Res Aug 1;2006 12(15):4590–4597. [PubMed: 16899606]
68. Yang YJ, Ryu JS, Kim SY, et al. Use of 3′-deoxy-3′-[18F]fluorothymidine PET to monitor early responses to radiation therapy in murine SCCVII tumors. Eur J Nucl Med Mol Imaging Apr 2006;33 (4):412–419.
69. Sun H, Sloan A, Mangner TJ, et al. Imaging DNA synthesis with [(18)F]FMAU and positron emission tomography in patients with cancer. Eur J Nucl Med Mol Imaging Jan 2005;32(1):15–22.
70. Nimmagadda S, Mangner TJ, Sun H, et al. Biodistribution and Radiation Dosimetry Estimates of 1-(2′-Deoxy-2′-18F-Fluoro-1-{beta}-D-Arabinofuranosyl)-5-Bromouracil: PET Imaging Studies in Dogs. J Nucl Med Nov 2005;46(11):1916–1922.
71. Glunde K, Jacobs MA, Bhujwalla ZM. Choline metabolism in cancer: implications for diagnosis and therapy. Expert Rev Mol Diagn Nov 2006;6(6):821–829.
72. Zheng QH, Stone KL, Mock BH, et al. [11C]Choline as a potential PET marker for imaging of breast cancer athymic mice. Nucl Med Biol Nov 2002;29(8):803–807.
73. Hara T, Kosaka N, Kishi H. PET imaging of prostate cancer using carbon-11-choline. J Nucl Med Jun 1998;39(6):990–995.
74. Hara T, Kosaka N, Shinoura N, Kondo T. PET imaging of brain tumor with [methyl-11C]choline. J Nucl Med Jun 1997;38(6):842–847.
75. DeGrado TR, Baldwin SW, Wang S, et al. Synthesis and evaluation of (18)F-labeled choline analogs as oncologic PET tracers. J Nucl Med Dec 2001;42(12):1805–1814.
76. DeGrado TR, Coleman RE, Wang S, et al. Synthesis and evaluation of 18F-labeled choline as an oncologic tracer for positron emission tomography: initial findings in prostate cancer. Cancer Res Jan 1;2001 61(1):110–117. [PubMed: 11196147]
77. Hara T, Bansal A, Degrado TR. Choline transporter as a novel target for molecular imaging of cancer. Mol Imaging Oct–Dec;2006 5(4):498–509. [PubMed: 17150162]
78. Breeuwsma AJ, Pruim J, Jongen MM, et al. In vivo uptake of [11C]choline does not correlate with cell proliferation in human prostate cancer. Eur J Nucl Med Mol Imaging Jun;2005 32(6):668–673. [PubMed: 15765234]
79. Al-Saeedi F, Welch AE, Smith TA. [methyl-3H]Choline incorporation into MCF7 tumour cells: correlation with proliferation. Eur J Nucl Med Mol Imaging Jun;2005 32(6):660–667. [PubMed: 15660258]
80. Pathak AP, Gimi B, Glunde K, Ackerstaff E, Artemov D, Bhujwalla ZM. Molecular and functional imaging of cancer: advances in MRI and MRS. Methods Enzymol 2004;386:3–60. [PubMed: 15120245]
81. Gillies RJ, Morse DL. In vivo magnetic resonance spectroscopy in cancer. Annu Rev Biomed Eng 2005;7:287–326. [PubMed: 16004573]
82. Glunde K, Ackerstaff E, Mori N, Jacobs MA, Bhujwalla ZM. Choline phospholipid metabolism in cancer: consequences for molecular pharmaceutical interventions. Mol Pharm Sep–Oct;2006 3(5): 496–506. [PubMed: 17009848]
83. Lichy MP, Bachert P, Hamprecht F, et al. [Application of (1)H MR spectroscopic imaging in radiation oncology: choline as a marker for determining the relative probability of tumor progression after radiation of glial brain tumors]. Rofo Jun;2006 178(6):627–633. [PubMed: 16703499]
84. Zeng QS, Li CF, Liu H, Zhen JH, Feng DC. Distinction between recurrent glioma and radiation injury using magnetic resonance spectroscopy in combination with diffusion-weighted imaging. Int J Radiat Oncol Biol Phys May 1;2007 68(1):151–158. [PubMed: 17289287]
85. Chao KS, Bosch WR, Mutic S, et al. A novel approach to overcome hypoxic tumor resistance: Cu-ATSM-guided intensity-modulated radiation therapy. Int J Radiat Oncol Biol Phys Mar 15;2001 49 (4):1171–1182. [PubMed: 11240261]

NIH-PA Author Manuscript

NIH-PA Author Manuscript

NIH-PA Author Manuscript

86. Popple RA, Ove R, Shen S. Tumor control probability for selective boosting of hypoxic subvolumes, including the effect of reoxygenation. Int J Radiat Oncol Biol Phys Nov 1;2002 54(3):921–927. [PubMed: 12377346]

87. Bussink J, Kaanders JH, Rijken PF, Raleigh JA, Van der Kogel AJ. Changes in blood perfusion and hypoxia after irradiation of a human squamous cell carcinoma xenograft tumor line. Radiat Res Apr; 2000 153(4):398–404. [PubMed: 10760999]

88. Cowen RL, Williams KJ, Chinje EC, et al. Hypoxia targeted gene therapy to increase the efficacy of tirapazamine as an adjuvant to radiotherapy: reversing tumor radioresistance and effecting cure. Cancer Res Feb 15;2004 64(4):1396–1402. [PubMed: 14973055]

89. Greco O, Joiner MC, Doleh A, Powell AD, Hillman GG, Scott SD. Hypoxia- and radiation-activated Cre/loxP 'molecular switch' vectors for gene therapy of cancer. Gene Ther Feb;2006 13(3):206–215. [PubMed: 16307003]

90. Lipnik K, Greco O, Scott S, et al. Hypoxia- and radiation-inducible, breast cell-specific targeting of retroviral vectors. Virology May 25;2006 349(1):121–133. [PubMed: 16464484]

91. Padhani AR, Krohn KA, Lewis JS, Alber M. Imaging oxygenation of human tumours. Eur Radiol Apr;2007 17(4):861–872. [PubMed: 17043737]

92. Rajendran JG, Krohn KA. Imaging hypoxia and angiogenesis in tumors. Radiol Clin North Am Jan; 2005 43(1):169–187. [PubMed: 15693655]

93. Rajendran JG, Schwartz DL, O'Sullivan J, et al. Tumor hypoxia imaging with [F-18] fluoromisonidazole positron emission tomography in head and neck cancer. Clin Cancer Res Sep 15;2006 12(18):5435–5441. [PubMed: 17000677]

94. Nordsmark M, Bentzen SM, Rudat V, et al. Prognostic value of tumor oxygenation in 397 head and neck tumors after primary radiation therapy. An international multi-center study. Radiother Oncol Oct;2005 77(1):18–24. [PubMed: 16098619]

95. Dubois L, Landuyt W, Haustermans K, et al. Evaluation of hypoxia in an experimental rat tumour model by [(18)F]fluoromisonidazole PET and immunohistochemistry. Br J Cancer Nov 29;2004 91 (11):1947–1954. [PubMed: 15520822]

96. Koh WJ, Bergman KS, Rasey JS, et al. Evaluation of oxygenation status during fractionated radiotherapy in human nonsmall cell lung cancers using [F-18]fluoromisonidazole positron emission tomography. Int J Radiat Oncol Biol Phys Sep 30;1995 33(2):391–398. [PubMed: 7673026]

97. Rajendran JG, Mankoff DA, O'Sullivan F, et al. Hypoxia and glucose metabolism in malignant tumors: evaluation by [18F]fluoromisonidazole and [18F]fluorodeoxyglucose positron emission tomography imaging. Clin Cancer Res Apr 1;2004 10(7):2245–2252. [PubMed: 15073099]

98. Rajendran JG, Wilson DC, Conrad EU, et al. [(18)F]FMISO and [(18)F]FDG PET imaging in soft tissue sarcomas: correlation of hypoxia, metabolism and VEGF expression. Eur J Nucl Med Mol Imaging May;2003 30(5):695–704. [PubMed: 12632200]

99. Cook GJ, Houston S, Barrington SF, Fogelman I. Technetium-99m-labeled HL91 to identify tumor hypoxia: correlation with fluorine-18-FDG. J Nucl Med Jan;1998 39(1):99–103. [PubMed: 9443745]

100. Zhang X, Melo T, Ballinger JR, Rauth AM. Studies of 99mTc-BnAO (HL-91): a non-nitroaromatic compound for hypoxic cell detection. Int J Radiat Oncol Biol Phys Nov 1;1998 42(4):737–740. [PubMed: 9845087]

101. Fujibayashi Y, Taniuchi H, Yonekura Y, Ohtani H, Konishi J, Yokoyama A. Copper-62-ATSM: a new hypoxia imaging agent with high membrane permeability and low redox potential. J Nucl Med Jul;1997 38(7):1155–1160. [PubMed: 9225812]

102. Dehdashti F, Mintun MA, Lewis JS, et al. In vivo assessment of tumor hypoxia in lung cancer with 60Cu-ATSM. Eur J Nucl Med Mol Imaging Jun;2003 30(6):844–850. [PubMed: 12692685]

103. Dehdashti F, Grigsby PW, Mintun MA, Lewis JS, Siegel BA, Welch MJ. Assessing tumor hypoxia in cervical cancer by positron emission tomography with 60Cu-ATSM: relationship to therapeutic response-a preliminary report. Int J Radiat Oncol Biol Phys Apr 1;2003 55(5):1233–1238. [PubMed: 12654432]

104. Matsumoto K, Szajek L, Krishna MC, et al. The influence of tumor oxygenation on hypoxia imaging in murine squamous cell carcinoma using [64Cu]Cu-ATSM or [18F]Fluoromisonidazole positron emission tomography. Int J Oncol Apr;2007 30(4):873–881. [PubMed: 17332926]

NIH-PA Author Manuscript

NIH-PA Author Manuscript

NIH-PA Author Manuscript

105. Lewis J, Laforest R, Buettner T, et al. Copper-64-diacetyl-bis(N4-methylthiosemicarbazone): An agent for radiotherapy. Proc Natl Acad Sci U S A Jan 30;2001 98(3):1206–1211. [PubMed: 11158618]
106. Obata A, Kasamatsu S, Lewis JS, et al. Basic characterization of 64Cu-ATSM as a radiotherapy agent. Nucl Med Biol Jan;2005 32(1):21–28. [PubMed: 15691658]
107. Aft RL, Lewis JS, Zhang F, Kim J, Welch MJ. Enhancing targeted radiotherapy by copper(II) diacetyl- bis(N4-methylthiosemicarbazone) using 2-deoxy-D-glucose. Cancer Res Sep 1;2003 63 (17):5496–5504. [PubMed: 14500386]
108. Burgman P, O'Donoghue JA, Lewis JS, Welch MJ, Humm JL, Ling CC. Cell line-dependent differences in uptake and retention of the hypoxia-selective nuclear imaging agent Cu-ATSM. Nucl Med Biol Aug;2005 32(6):623–630. [PubMed: 16026709]
109. Zanzonico P, O'Donoghue J, Chapman JD, et al. Iodine-124-labeled iodo- azomycin-galactoside imaging of tumor hypoxia in mice with serial microPET scanning. Eur J Nucl Med Mol Imaging Jan;2004 31(1):117–128. [PubMed: 14523586]
110. Beck R, Roper B, Carlsen JM, et al. Pretreatment 18F-FAZA PET predicts success of hypoxia-directed radiochemotherapy using tirapazamine. J Nucl Med Jun;2007 48(6):973–980. [PubMed: 17536108]
111. Brown JM, Attardi LD. The role of apoptosis in cancer development and treatment response. Nat Rev Cancer Mar;2005 5(3):231–237. [PubMed: 15738985]
112. Meyn RE, Stephens LC, Milas L. Programmed cell death and radioresistance. Cancer Metastasis Rev Mar;1996 15(1):119–131. [PubMed: 8842483]
113. Boersma HH, Kietselaer BL, Stolk LM, et al. Past, present, and future of annexin A5: from protein discovery to clinical applications. J Nucl Med Dec;2005 46(12):2035–2050. [PubMed: 16330568]
114. Yagle KJ, Eary JF, Tait JF, et al. Evaluation of 18F-annexin V as a PET imaging agent in an animal model of apoptosis. J Nucl Med Apr;2005 46(4):658–666. [PubMed: 15809489]
115. Blankenberg FG, Katsikis PD, Tait JF, et al. Imaging of apoptosis (programmed cell death) with 99mTc annexin V. J Nucl Med Jan;1999 40(1):184–191. [PubMed: 9935075]
116. Keen HG, Dekker BA, Disley L, et al. Imaging apoptosis in vivo using 124I-annexin V and PET. Nucl Med Biol May;2005 32(4):395–402. [PubMed: 15878509]
117. Belhocine T, Steinmetz N, Hustinx R, et al. Increased uptake of the apoptosis-imaging agent (99m) Tc recombinant human Annexin V in human tumors after one course of chemotherapy as a predictor of tumor response and patient prognosis. Clin Cancer Res Sep;2002 8(9):2766–2774. [PubMed: 12231515]
118. Haas RL, de Jong D, Valdes Olmos RA, et al. In vivo imaging of radiation-induced apoptosis in follicular lymphoma patients. Int J Radiat Oncol Biol Phys Jul 1;2004 59(3):782–787. [PubMed: 15183481]
119. Petrovsky A, Schellenberger E, Josephson L, Weissleder R, Bogdanov A Jr. Near-infrared fluorescent imaging of tumor apoptosis. Cancer Res Apr 15;2003 63(8):1936–1942. [PubMed: 12702586]
120. Ntziachristos V, Schellenberger EA, Ripoll J, et al. Visualization of antitumor treatment by means of fluorescence molecular tomography with an annexin V-Cy5.5 conjugate. Proc Natl Acad Sci U S A Aug 17;2004 101(33):12294–12299. [PubMed: 15304657]
121. Davletov BA, Sudhof TC. A single C2 domain from synaptotagmin I is sufficient for high affinity Ca2+/phospholipid binding. J Biol Chem Dec 15;1993 268(35):26386–26390. [PubMed: 8253763]
122. Zhao M, Beauregard DA, Loizou L, Davletov B, Brindle KM. Non-invasive detection of apoptosis using magnetic resonance imaging and a targeted contrast agent. Nat Med Nov;2001 7(11):1241–1244. [PubMed: 11689890]
123. Massie C, Mills IG. The developing role of receptors and adaptors. Nat Rev Cancer May;2006 6(5): 403–409. [PubMed: 16612404]
124. Srinivasan DM, Kapoor M, Kojima F, Crofford LJ. Growth factor receptors: implications in tumor biology. Curr Opin Investig Drugs Dec;2005 6(12):1246–1249.
125. Osborne CK. Tamoxifen in the treatment of breast cancer. N Engl J Med Nov 26;1998 339(22): 1609–1618. [PubMed: 9828250]

NIH-PA Author Manuscript

NIH-PA Author Manuscript

NIH-PA Author Manuscript

126. Linden HM, Stekhova SA, Link JM, et al. Quantitative fluoroestradiol positron emission tomography imaging predicts response to endocrine treatment in breast cancer. J Clin Oncol Jun 20;2006 24 (18):2793–2799. [PubMed: 16682724]

127. Dehdashti F, Mortimer JE, Siegel BA, et al. Positron tomographic assessment of estrogen receptors in breast cancer: comparison with FDG-PET and in vitro receptor assays. J Nucl Med Oct;1995 36 (10):1766–1774. [PubMed: 7562040]

128. Dehdashti F, Picus J, Michalski JM, et al. Positron tomographic assessment of androgen receptors in prostatic carcinoma. Eur J Nucl Med Mol Imaging Mar;2005 32(3):344–350. [PubMed: 15726353]

129. Iznaga-Escobar N, Torres LA, Morales A, et al. Technetium-99m-labeled anti-EGF-receptor antibody in patients with tumor of epithelial origin: I. Biodistribution and dosimetry for radioimmunotherapy. J Nucl Med Jan;1998 39(1):15–23. [PubMed: 9443731]

130. Ramos-Suzarte M, Rodriguez N, Oliva JP, et al. 99mTc-labeled antihuman epidermal growth factor receptor antibody in patients with tumors of epithelial origin: Part III. Clinical trials safety and diagnostic efficacy. J Nucl Med May;1999 40(5):768–775. [PubMed: 10319748]

131. Ke S, Wen X, Gurfinkel M, et al. Near-infrared optical imaging of epidermal growth factor receptor in breast cancer xenografts. Cancer Res Nov 15;2003 63(22):7870–7875. [PubMed: 14633715]

132. Mishani E, Abourbeh G, Rozen Y, et al. Novel carbon-11 labeled 4-dimethylamino-but-2-enoic acid [4-(phenylamino)-quinazoline-6-yl]-amides: potential PET bioprobes for molecular imaging of EGFR-positive tumors. Nucl Med Biol May;2004 31(4):469–476. [PubMed: 15093817]

133. Pal A, Glekas A, Doubrovin M, et al. Molecular imaging of EGFR kinase activity in tumors with 124I-labeled small molecular tracer and positron emission tomography. Mol Imaging Biol Sep-Oct; 2006 8(5):262–277. [PubMed: 16897320]

134. Wang JQ, Gao M, Miller KD, Sledge GW, Zheng QH. Synthesis of [11C]Iressa as a new potential PET cancer imaging agent for epidermal growth factor receptor tyrosine kinase. Bioorg Med Chem Lett Aug 1;2006 16(15):4102–4106. [PubMed: 16697188]

135. Hynes NE, Lane HA. ERBB receptors and cancer: the complexity of targeted inhibitors. Nat Rev Cancer May;2005 5(5):341–354. [PubMed: 15864276]

136. Cooke T, Reeves J, Lanigan A, Stanton P. HER2 as a prognostic and predictive marker for breast cancer. Ann Oncol 2001;12 Suppl 1:S23–28. [PubMed: 11521717]

137. Robinson MK, Doss M, Shaller C, et al. Quantitative immuno-positron emission tomography imaging of HER2-positive tumor xenografts with an iodine-124 labeled anti-HER2 diabody. Cancer Res Feb 15;2005 65(4):1471–1478. [PubMed: 15735035]

138. Perik PJ, Lub-De Hooge MN, Gietema JA, et al. Indium-111-labeled trastuzumab scintigraphy in patients with human epidermal growth factor receptor 2-positive metastatic breast cancer. J Clin Oncol May 20;2006 24(15):2276–2282. [PubMed: 16710024]

139. Krenning EP, Bakker WH, Kooij PP, et al. Somatostatin receptor scintigraphy with indium-111-DTPA-D-Phe-1-octreotide in man: metabolism, dosimetry and comparison with iodine-123-Tyr-3-octreotide. J Nucl Med May;1992 33(5):652–658. [PubMed: 1349039]

140. Anderson CJ, Dehdashti F, Cutler PD, et al. 64Cu-TETA-octreotide as a PET imaging agent for patients with neuroendocrine tumors. J Nucl Med Feb;2001 42(2):213–221. [PubMed: 11216519]

141. Henze M, Schuhmacher J, Hipp P, et al. PET imaging of somatostatin receptors using [68GA]DOTA-D-Phe1-Tyr3-octreotide: first results in patients with meningiomas. J Nucl Med Jul;2001 42(7): 1053–1056. [PubMed: 11438627]

142. Gabriel M, Decristoforo C, Kendler D, et al. 68Ga-DOTA-Tyr3-Octreotide PET in Neuroendocrine Tumors: Comparison with Somatostatin Receptor Scintigraphy and CT. J Nucl Med Apr;2007 48 (4):508–518. [PubMed: 17401086]

143. Moore A, Josephson L, Bhorade RM, Basilion JP, Weissleder R. Human transferrin receptor gene as a marker gene for MR imaging. Radiology Oct;2001 221(1):244–250. [PubMed: 11568347]

144. Artemov D, Mori N, Okollie B, Bhujwalla ZM. MR molecular imaging of the Her-2/neu receptor in breast cancer cells using targeted iron oxide nanoparticles. Magn Reson Med Mar;2003 49(3): 403–408. [PubMed: 12594741]

145. Artemov D, Mori N, Ravi R, Bhujwalla ZM. Magnetic resonance molecular imaging of the HER-2/neu receptor. Cancer Res Jun 1;2003 63(11):2723–2727. [PubMed: 12782573]

NIH-PA Author Manuscript

NIH-PA Author Manuscript

NIH-PA Author Manuscript

146. Penuelas I, Haberkorn U, Yaghoubi S, Gambhir SS. Gene therapy imaging in patients for oncological applications. Eur J Nucl Med Mol Imaging Dec;2005 32 Suppl 2:S384–403. [PubMed: 16180032]

147. Niu G, Gaut AW, Ponto LL, et al. Multimodality noninvasive imaging of gene transfer using the human sodium iodide symporter. J Nucl Med Mar;2004 45(3):445–449. [PubMed: 15001685]

148. Groot-Wassink T, Aboagye EO, Wang Y, Lemoine NR, Reader AJ, Vassaux G. Quantitative imaging of Na/I symporter transgene expression using positron emission tomography in the living animal. Mol Ther Mar;2004 9(3):436–442. [PubMed: 15006611]

149. Liang Q, Satyamurthy N, Barrio JR, et al. Noninvasive, quantitative imaging in living animals of a mutant dopamine D2 receptor reporter gene in which ligand binding is uncoupled from signal transduction. Gene Ther Oct;2001 8(19):1490–1498. [PubMed: 11593362]

150. MacLaren DC, Gambhir SS, Satyamurthy N, et al. Repetitive, non-invasive imaging of the dopamine D2 receptor as a reporter gene in living animals. Gene Ther May;1999 6(5):785–791. [PubMed: 10505102]

151. Tjuvajev JG, Stockhammer G, Desai R, et al. Imaging the expression of transfected genes in vivo. Cancer Res Dec 15;1995 55(24):6126–6132. [PubMed: 8521403]

152. Tjuvajev JG, Avril N, Oku T, et al. Imaging herpes virus thymidine kinase gene transfer and expression by positron emission tomography. Cancer Res 1998;58(19):4333–4341. [PubMed: 9766661]

153. Gambhir SS, Bauer E, Black ME, et al. A mutant herpes simplex virus type 1 thymidine kinase reporter gene shows improved sensitivity for imaging reporter gene expression with positron emission tomography. Proc Natl Acad Sci U S A 2000;97(6):2785–2790. [PubMed: 10716999]

154. Yaghoubi SS, Wu L, Liang Q, et al. Direct correlation between positron emission tomographic images of two reporter genes delivered by two distinct adenoviral vectors. Gene Ther Jul;2001 8 (14):1072–1080. [PubMed: 11526454]

155. Qiao J, Doubrovin M, Sauter BV, et al. Tumor-specific transcriptional targeting of suicide gene therapy. Gene Ther Feb;2002 9(3):168–175. [PubMed: 11859419]

156. Doubrovin M, Ponomarev V, Beresten T, et al. Imaging transcriptional regulation of p53-dependent genes with positron emission tomography in vivo. Proc Natl Acad Sci U S A Jul 31;2001 98(16): 9300–9305. [PubMed: 11481488]

157. Bhaumik S, Walls Z, Puttaraju M, Mitchell LG, Gambhir SS. Molecular imaging of gene expression in living subjects by spliceosome-mediated RNA trans-splicing. Proc Natl Acad Sci U S A Jun 8;2004 101(23):8693–8698. [PubMed: 15161977]

158. Luker GD, Sharma V, Pica CM, Prior JL, Li W, Piwnica-Worms D. Molecular imaging of protein-protein interactions: controlled expression of p53 and large T-antigen fusion proteins in vivo. Cancer Res Apr 15;2003 63(8):1780–1788. [PubMed: 12702563]

159. Shu CJ, Guo S, Kim YJ, et al. Visualization of a primary anti-tumor immune response by positron emission tomography. Proc Natl Acad Sci U S A Nov 29;2005 102(48):17412–17417. [PubMed: 16293690]

160. Penuelas I, Mazzolini G, Boan JF, et al. Positron emission tomography imaging of adenoviral-mediated transgene expression in liver cancer patients. Gastroenterology Jun;2005 128(7):1787–1795. [PubMed: 15940613]

161. Fu DX, Tanhehco YC, Chen J, et al. Virus-associated tumor imaging by induction of viral gene expression. Clin Cancer Res Mar 1;2007 13(5):1453–1458. [PubMed: 17332288]

162. Moeller BJ, Richardson RA, Dewhirst MW. Hypoxia and radiotherapy: opportunities for improved outcomes in cancer treatment. Cancer Metastasis Rev Jun;2007 26(2):241–248. [PubMed: 17440683]

163. Greco O, Marples B, Dachs GU, Williams KJ, Patterson AV, Scott SD. Novel chimeric gene promoters responsive to hypoxia and ionizing radiation. Gene Ther Oct;2002 9(20):1403–1411. [PubMed: 12365006]

164. Cohen B, Dafni H, Meir G, Harmelin A, Neeman M. Ferritin as an endogenous MRI reporter for noninvasive imaging of gene expression in C6 glioma tumors. Neoplasia Feb;2005 7(2):109–117. [PubMed: 15802016]

165. Genove G, DeMarco U, Xu H, Goins WF, Ahrens ET. A new transgene reporter for in vivo magnetic resonance imaging. Nat Med Apr;2005 11(4):450–454. [PubMed: 15778721]

NIH-PA Author Manuscript

NIH-PA Author Manuscript

NIH-PA Author Manuscript

166. Gilad AA, McMahon MT, Walczak P, et al. Artificial reporter gene providing MRI contrast based on proton exchange. Nat Biotechnol Feb;2007 25(2):217–219. [PubMed: 17259977]

167. Fidler IJ, Ellis LM. The implications of angiogenesis for the biology and therapy of cancer metastasis. Cell Oct 21;1994 79(2):185–188. [PubMed: 7525076]

168. Folkman J. Angiogenesis in cancer, vascular, rheumatoid and other disease. Nat Med Jan;1995 1 (1):27–31. [PubMed: 7584949]

169. Shaked Y, Kerbel RS. Antiangiogenic strategies on defense: on the possibility of blocking rebounds by the tumor vasculature after chemotherapy. Cancer Res Aug 1;2007 67(15):7055–7058. [PubMed: 17671170]

170. Folkman J. Angiogenesis: an organizing principle for drug discovery? Nat Rev Drug Discov Apr; 2007 6(4):273–286. [PubMed: 17396134]

171. Leach MO, Brindle KM, Evelhoch JL, et al. The assessment of antiangiogenic and antivascular therapies in early-stage clinical trials using magnetic resonance imaging: issues and recommendations. Br J Cancer May 9;2005 92(9):1599–1610. [PubMed: 15870830]

172. Kiessling F, Greschus S, Lichy MP, et al. Volumetric computed tomography (VCT): a new technology for noninvasive, high-resolution monitoring of tumor angiogenesis. Nat Med Oct;2004 10(10):1133–1138. [PubMed: 15361864]

173. Cai W, Rao J, Gambhir SS, Chen X. How molecular imaging is speeding up antiangiogenic drug development. Mol Cancer Ther Nov;2006 5(11):2624–2633. [PubMed: 17121909]

174. Tabruyn SP, Griffioen AW. Molecular pathways of angiogenesis inhibition. Biochem Biophys Res Commun Mar 30;2007 355(1):1–5. [PubMed: 17276388]

175. Ferrara N. VEGF and the quest for tumour angiogenesis factors. Nat Rev Cancer Oct;2002 2(10): 795–803. [PubMed: 12360282]

176. Cai W, Chen K, Mohamedali KA, et al. PET of vascular endothelial growth factor receptor expression. J Nucl Med Dec;2006 47(12):2048–2056. [PubMed: 17138749]

177. Blankenberg FG, Backer MV, Levashova Z, Patel V, Backer JM. In vivo tumor angiogenesis imaging with site-specific labeled (99m)Tc-HYNIC-VEGF. Eur J Nucl Med Mol Imaging Jul;2006 33(7): 841–848. [PubMed: 16699765]

178. Blankenberg FG, Mandl S, Cao YA, et al. Tumor imaging using a standardized radiolabeled adapter protein docked to vascular endothelial growth factor. J Nucl Med Aug;2004 45(8):1373–1380. [PubMed: 15299064]

179. Cornelissen B, Oltenfreiter R, Kersemans V, et al. In vitro and in vivo evaluation of [123I]-VEGF165 as a potential tumor marker. Nucl Med Biol Jul;2005 32(5):431–436. [PubMed: 15982572]

180. Jayson GC, Zweit J, Jackson A, et al. Molecular imaging and biological evaluation of HuMV833 anti-VEGF antibody: implications for trial design of antiangiogenic antibodies. J Natl Cancer Inst Oct 2;2002 94(19):1484–1493. [PubMed: 12359857]

181. Hood JD, Cheresh DA. Role of integrins in cell invasion and migration. Nat Rev Cancer Feb;2002 2(2):91–100. [PubMed: 12635172]

182. Stupack DG, Cheresh DA. Integrins and angiogenesis. Curr Top Dev Biol 2004;64:207–238. [PubMed: 15563949]

183. Liu S. Radiolabeled multimeric cyclic RGD peptides as integrin alphavbeta3 targeted radiotracers for tumor imaging. Mol Pharm Sep–Oct;2006 3(5):472–487. [PubMed: 17009846]

184. Beer AJ, Haubner R, Sarbia M, et al. Positron emission tomography using [18F]Galacto-RGD identifies the level of integrin alpha(v)beta3 expression in man. Clin Cancer Res Jul 1;2006 12(13): 3942–3949. [PubMed: 16818691]

185. Haubner R, Weber WA, Beer AJ, et al. Noninvasive visualization of the activated alphavbeta3 integrin in cancer patients by positron emission tomography and [18F]Galacto-RGD. PLoS Med Mar;2005 2(3):e70. [PubMed: 15783258]

186. Winter PM, Caruthers SD, Kassner A, et al. Molecular imaging of angiogenesis in nascent Vx-2 rabbit tumors using a novel alpha(nu)beta3-targeted nanoparticle and 1.5 tesla magnetic resonance imaging. Cancer Res Sep 15;2003 63(18):5838–5843. [PubMed: 14522907]

187. Sipkins DA, Cheresh DA, Kazemi MR, Nevin LM, Bednarski MD, Li KC. Detection of tumor angiogenesis in vivo by alphaVbeta3-targeted magnetic resonance imaging. Nat Med May;1998 4 (5):623–626. [PubMed: 9585240]

NIH-PA Author Manuscript

NIH-PA Author Manuscript

NIH-PA Author Manuscript

188. Anderson SA, Rader RK, Westlin WF, et al. Magnetic resonance contrast enhancement of neovasculature with alpha(v)beta(3)-targeted nanoparticles. Magn Reson Med Sep;2000 44(3): 433–439. [PubMed: 10975896]
189. Chen X, Conti PS, Moats RA. In vivo near-infrared fluorescence imaging of integrin alphavbeta3 in brain tumor xenografts. Cancer Res Nov 1;2004 64(21):8009–8014. [PubMed: 15520209]
190. Ellegala DB, Leong-Poi H, Carpenter JE, et al. Imaging tumor angiogenesis with contrast ultrasound and microbubbles targeted to alpha(v)beta3. Circulation Jul 22;2003 108(3):336–341. [PubMed: 12835208]
191. Deryugina EI, Quigley JP. Matrix metalloproteinases and tumor metastasis. Cancer Metastasis Rev Mar;2006 25(1):9–34. [PubMed: 16680569]
192. Overall CM, Lopez-Otin C. Strategies for MMP inhibition in cancer: innovations for the post-trial era. Nat Rev Cancer Sep;2002 2(9):657–672. [PubMed: 12209155]
193. Van de Wiele C, Oltenfreiter R. Imaging probes targeting matrix metalloproteinases. Cancer Biother Radiopharm Oct;2006 21(5):409–417. [PubMed: 17105415]
194. Choe YS, Lee KH. Targeted in vivo imaging of angiogenesis: present status and perspectives. Curr Pharm Des 2007;13(1):17–31. [PubMed: 17266586]
195. Furumoto S, Takashima K, Kubota K, Ido T, Iwata R, Fukuda H. Tumor detection using 18F-labeled matrix metalloproteinase-2 inhibitor. Nucl Med Biol Feb;2003 30(2):119–125. [PubMed: 12623110]
196. Giersing BK, Rae MT, CarballidoBrea M, Williamson RA, Blower PJ. Synthesis and characterization of 111In-DTPA-N-TIMP-2: a radiopharmaceutical for imaging matrix metalloproteinase expression. Bioconjug Chem Nov–Dec;2001 12(6):964–971. [PubMed: 11716687]
197. Medina OP, Kairemo K, Valtanen H, et al. Radionuclide imaging of tumor xenografts in mice using a gelatinase-targeting peptide. Anticancer Res Jan-Feb;2005 25(1A):33–42. [PubMed: 15816516]
198. Bremer C, Tung CH, Weissleder R. In vivo molecular target assessment of matrix metalloproteinase inhibition. Nat Med Jun;2001 7(6):743–748. [PubMed: 11385514]
199. Mahmood U, Weissleder R. Near-infrared optical imaging of proteases in cancer. Mol Cancer Ther May;2003 2(5):489–496. [PubMed: 12748311]
200. Funovics M, Montet X, Reynolds F, Weissleder R, Josephson L. Nanoparticles for the optical imaging of tumor E-selectin. Neoplasia Oct;2005 7(10):904–911. [PubMed: 16242073]
201. Yang DJ, Kim KD, Schechter NR, et al. Assessment of antiangiogenic effect using 99mTc-EC-endostatin. Cancer Biother Radiopharm Apr;2002 17(2):233–245. [PubMed: 12030117]
202. Nyati MK, Morgan MA, Feng FY, Lawrence TS. Integration of EGFR inhibitors with radiochemotherapy. Nat Rev Cancer Nov;2006 6(11):876–885. [PubMed: 17036041]
203. Hicke BJ, Stephens AW, Gould T, et al. Tumor targeting by an aptamer. J Nucl Med Apr;2006 47 (4):668–678. [PubMed: 16595502]
204. Lappin G, Garner RC. Big physics, small doses: the use of AMS and PET in human microdosing of development drugs. Nat Rev Drug Discov Mar;2003 2(3):233–240. [PubMed: 12612650]
205. Kummar S, Kinders R, Rubinstein L, et al. Compressing drug development timelines in oncology using phase ‘0’ trials. Nat Rev Cancer Feb;2007 7(2):131–139. [PubMed: 17251919]
206. Jacobs A, Voges J, Reszka R, et al. Positron-emission tomography of vector-mediated gene expression in gene therapy for gliomas. Lancet 2001;358:727–729. [PubMed: 11551583]

NIH-PA Author Manuscript

NIH-PA Author Manuscript

NIH-PA Author Manuscript

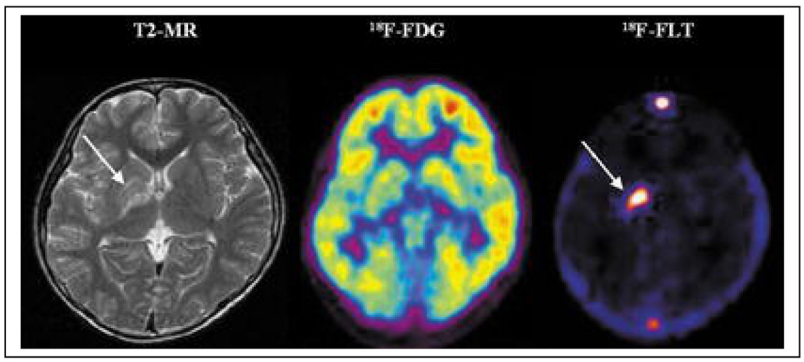

Figure 1. Comparison of FDG and FLT

An 11-year-old male with a germ cell tumor of the basal ganglia. MRI shows subtle changes (*arrow*) in the right basal ganglia. On FDG-PET, the right basal ganglia lesion shows slightly decreased uptake compared with the contralateral basal ganglia but increased uptake compared with normal white matter. 3′-Deoxy-3′-[^{18}F]fluorothymidine (FLT)-PET, however, reveals intensely increased uptake, suggesting the presence of a malignant tumor (*arrow*). Based on the FLT-PET results, a stereotactic biopsy was performed in the right putamen. could be performed in the right basal ganglia (63).

From: Choi SJ, Kim JS, Kim JH, et al. [18F]3′-deoxy-3′-fluorothymidine PET for the diagnosis and grading of brain tumors. *Eur J Nucl Med Mol Imaging.* Jun 2005;32(6):653–659.

NIH-PA Author Manuscript
NIH-PA Author Manuscript
NIH-PA Author Manuscript

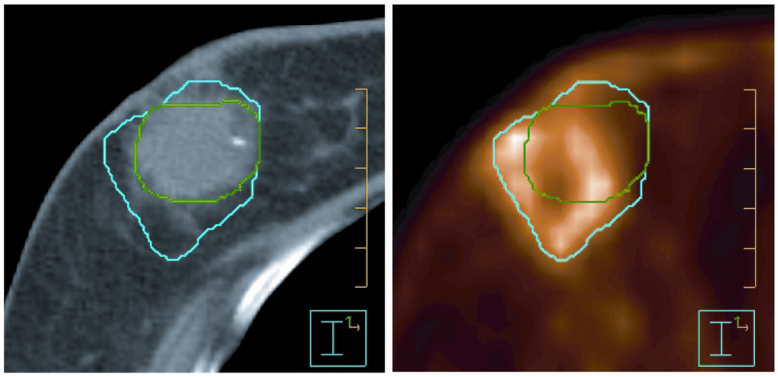

Figure 2.
Representative axial slices from CT (left) and FDG-PET (right) scans of a breast cancer patient after lumpectomy surgery. The lumpectomy cavity was delineated for further treatment with the partial breast irradiation technique. Contours based on FDG-PET-CT (blue) were generally larger than those defined on CT alone (green). (From Ford et al., 2007).

NIH-PA Author Manuscript
NIH-PA Author Manuscript
NIH-PA Author Manuscript

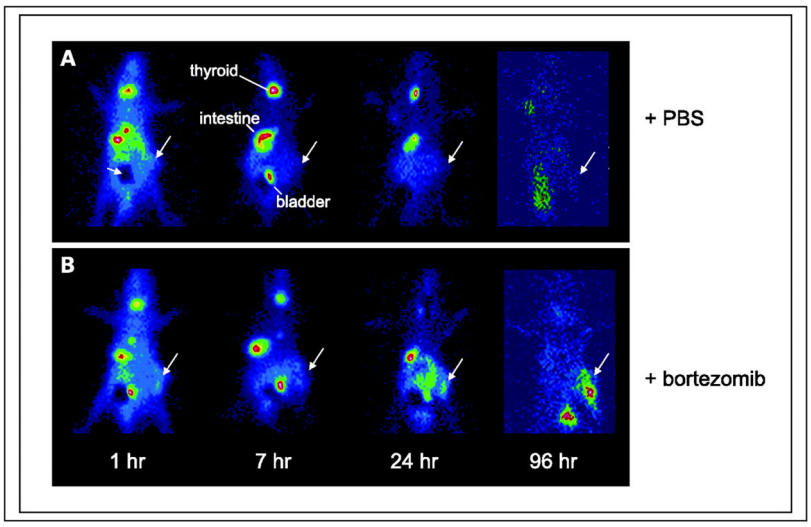

Figure 3. Viral TK induction

Time course of uptake of [^{125}I]FIAU by Burkitt's lymphoma xenografts [EBV(+) Akata] following treatment with bortezomib as assessed by planar gamma scintigraphy *in vivo*. Large arrows, tumors. The dark area (*A*, *small arrow*) represents lead shielding of bladder to improve the dynamic range of the images. Each animal has one tumor placed in the hind limb. *A*, no tumor uptake is evident in animals pretreated with PBS only (control). *B*, tumors are visualized at later time points in the pretreated animals (2 μg/g bortezomib).

From: Fu DX, Tanhehco YC, Chen J, et al. Virus-associated tumor imaging by induction of viral gene expression. *Clin Cancer Res.* Mar 1 2007;13(5):1453–1458.

NIH-PA Author Manuscript

NIH-PA Author Manuscript

NIH-PA Author Manuscript

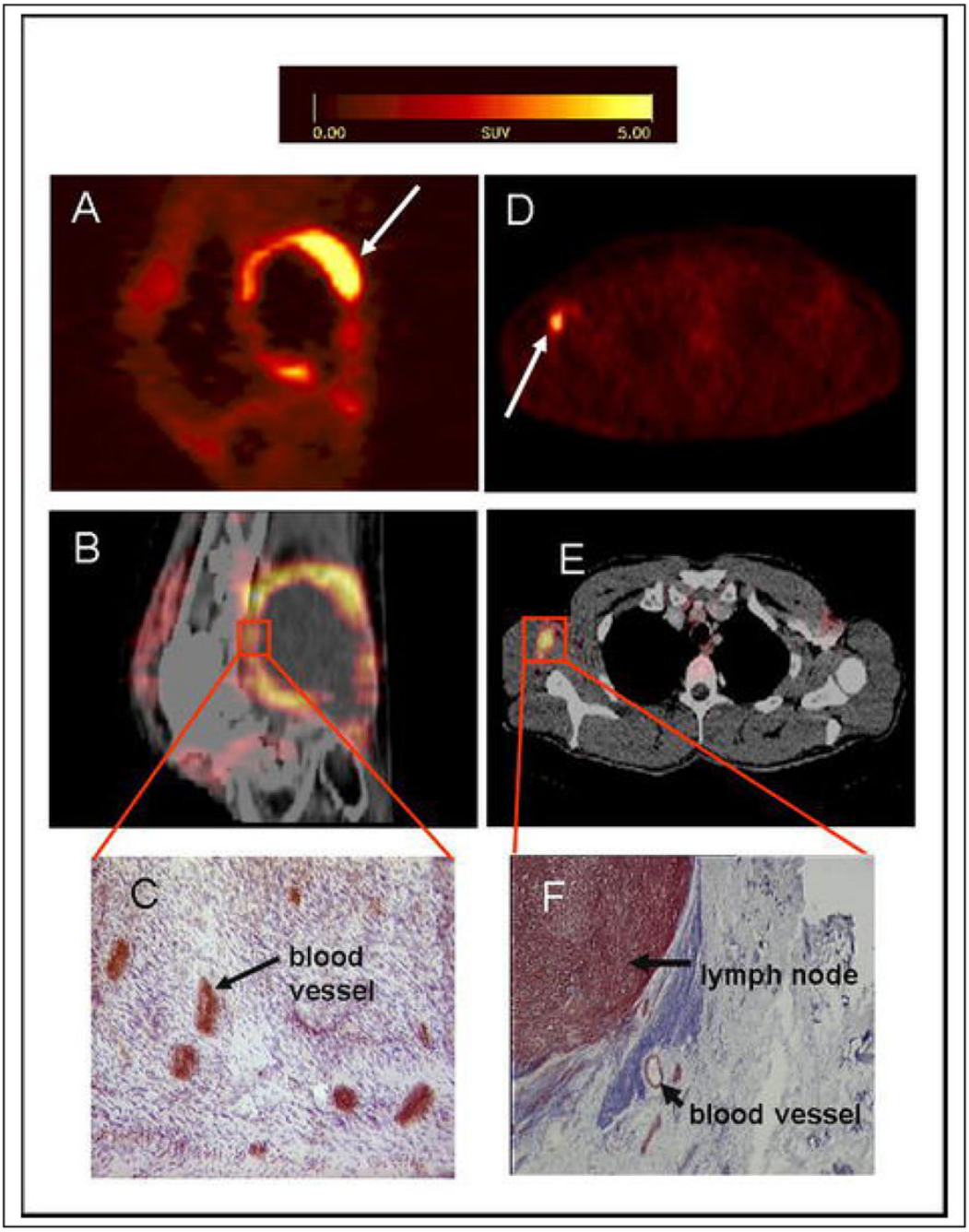

Figure 4. Correlation of tracer accumulation and $\alpha_v\beta_3$ expression

(A–C) patient with a soft tissue sarcoma dorsal of the right knee joint. (A) The sagittal section of a [^{18}F]galacto-RGD PET acquired 170 min p. i. shows circular peripheral tracer uptake in the tumor with variable intensity and a maximum SUV of 10.0 at the apical-dorsal aspect of the tumor (arrow). (B) The image fusion of the [^{18}F]galacto-RGD PET and the corresponding computed tomography scan after intravenous injection of contrast medium shows that the regions of intense tracer uptake correspond with the enhancing tumor wall, whereas the non-enhancing hypodense center of the tumor shows no tracer uptake. (C) Immunohistochemistry of a peripheral tumor section using the anti-αvβ3 monoclonal antibody LM609 demonstrates intense staining predominantly of tumor vasculature. (D–F) patient with malignant melanoma

NIH-PA Author Manuscript

NIH-PA Author Manuscript

NIH-PA Author Manuscript

and a lymph node metastasis in the right axilla. (D) The axial section of a [^{18}F]galacto-RGD PET acquired 140 min p. i. shows intense focal uptake in the lymph node (arrow). (E) Image fusion of the [^{18}F]galacto-RGD PET and the corresponding computed tomography scan after intravenous injection of contrast medium. (F) Immunohistochemistry of the lymph node using the anti-αvβ3 monoclonal antibody LM609 demonstrates intense staining predominantly of tumor cells and also blood vessels.

From: Noninvasive Visualization of the Activated αvβ3 Integrin in Cancer Patients by Positron Emission Tomography and [18F]Galacto-RGD Haubner R, Weber WA, Beer AJ, Vabuliene E, Reim D, et al. PLoS Medicine Vol. 2, No. 3, e70 doi:10.1371/journal.pmed.0020070